CHEMISTRY
A EUROPEAN JOURNAL

DOI: 10.1002/chem.200701615

Redox-Active *p*-Quinone-Based Bis(pyrazol-1-yl)methane Ligands: Synthesis and Coordination Behaviour

Sebastian Scheuermann,[a] Tonia Kretz,[a] Hannes Vitze,[a] Jan W. Bats,[b] Michael Bolte,[a] Hans-Wolfram Lerner,[a] and Matthias Wagner*[a]

Dedicated to Professor Dr. Wolfgang A. Herrmann on the occasion of his 60th birthday

Abstract: The synthesis, structural characterisation and coordination behaviour of mono- and ditopic *p*-hydroquinone-based bis(pyrazol-1-yl)methane ligands is described (i.e., 2-(pz_2CH)$C_6H_3(OH)_2$ (**2a**), 2-(pz_2CH)-6-(*t*Bu)$C_6H_2(OH)_2$ (**2b**), 2-(pz_2CH)-6-(*t*Bu)C_6H_2(OSi*i*Pr_3)(OH) (**2c**), 2,5-($pz_2CH)_2C_6H_2(OH)_2$ (**4**)). Ligands **2a**, **2b** and **4** can be oxidised to their *p*-benzoquinone state on a preparative scale (**2a**$_{ox}$, **2b**$_{ox}$, **4**$_{ox}$). An octahedral Ni^{II} complex [*trans*-Ni(**2c**)$_2$] and square-planar Pd^{II} complexes [Pd**2b**Cl_2] and [Pd**2b**$_{ox}Cl_2$] have been prepared. In the two Pd^{II} species, the ligands are coordinated only through their pyrazolyl rings. The fact that [Pd**2b**Cl_2] and [Pd**2b**$_{ox}Cl_2$] are isolable compounds proves that redox transitions involving the *p*-quinone substituent are fully reversible. In [Pd**2b**$_{ox}Cl_2$], the methine proton is highly acidic and can be abstracted with bases as weak as NEt_3. The resulting anion dimerises to give a dinuclear macrocyclic Pd^{II} complex, which has been structurally characterised. The methylated ligand 2-(pz_2CMe)$C_6H_3O_2$ (**11**$_{ox}$) and its Pd^{II} complex [Pd**11**$_{ox}Cl_2$] are base-stable. A new class of redox-active ligands is now available with the potential for applications both in catalysis and in materials science.

Keywords: ligand design · N,O ligands · palladium · pyrazolylmethanes · quinones

Introduction

The importance of transition-metal ions in homogeneous catalysis and materials science rests to a large extent on their ability to adopt different oxidation states. This redox capacity can be further enhanced by coordinating the metal ion with an electroactive ligand. Provided that the redox potential of the non-metal component matches that of the metal ion, the resulting complex is capable of undergoing multi-electron transfers that are the sum of the oxidation-state changes of the metal centre plus the redox changes of the ligand framework.[1]

Particularly impressive examples of the effectiveness of electroactive ligands in catalysis are provided by metalloenzymes like the Cyt-P450 systems in which a one-electron-oxidised porphyrinato ligand is present in the highly oxidised intermediate forms of the enzyme.[2]

In materials science, great attention is currently being paid to oligonuclear transition-metal aggregates with redox-active bridging units that are designed to have useful cooperative magnetic and electronic properties.[1,3,4]

Our group has a long-standing interest in the development of novel electroactive ligands both for use in homogeneous catalysis and in the assembly of coordination polymers and networks.[5] Initially we relied on ferrocene as a redox-active unit and prepared mono- and ditopic ferrocene-based poly(pyrazol-1-yl)borates $[FcB(Me)_npz_{3-n}]^-$ and $[fc\{B(Me)_npz_{3-n}\}_2]^{2-}$ (Fc = $(C_5H_5)Fe(C_5H_4)$, fc = $Fe(C_5H_4)_2$, pz = pyrazol-1-yl). Treatment of these ligands with metal ions (M^{n+}) gives discrete oligonuclear complexes, coordination polymers and multiple-decker sandwich complexes.[6–13] In some cases, cyclic voltammetric measurements indicate a dependence of the Fc/Fc^+ or fc/fc^+ redox potential on the

[a] S. Scheuermann, Dr. T. Kretz, H. Vitze, Dr. M. Bolte, Dr. H.-W. Lerner, Prof. Dr. M. Wagner
Institut für Anorganische und Analytische Chemie
Johann Wolfgang Goethe-Universität Frankfurt am Main
Max-von-Laue-Straße 7, 60438 Frankfurt (Germany)
Fax: (+49) 69-798-29260
E-mail: Matthias.Wagner@chemie.uni-frankfurt.de

[b] Dr. J. W. Bats
Institut für Organische Chemie und Chemische Biologie
Johann Wolfgang Goethe-Universität Frankfurt am Main
Max-von-Laue-Straße 7, 60438 Frankfurt (Germany)

Supporting information for this article is available on the WWW under http://www.chemeurj.org/ or from the author. It contains crystallographic characterisation of **2a**, **2b**$_{ox}$, **2c**, **4**·DMF_2 and **9**; synthesis, spectroscopic and crystallographic characterisation of **13** and cyclic voltammograms of **11**, **12** and **13**.

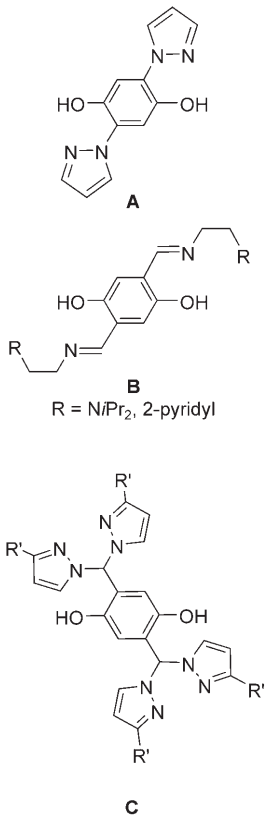

Figure 1. Redox-active, *p*-hydroquinone-based ditopic ligands: bidentate pyrazolyl ligand **A**, tridentate meridionally coordinating imine ligand **B** and tridentate facially coordinating bis(pyrazol-1-yl)methane ligand **C**.

oxidation state of M^{n+} (and vice versa), however, the degree of electronic communication is generally not very high.[7,9]

In the search for more strongly coupled systems, *o*- and *p*-quinone derivatives appeared to be particularly promising candidates as they are known to exist not only as closed-shell species, but also as reasonably stable radicals (cf. the *p*-hydroquinone/*p*-semiquinone/*p*-benzoquinone series; note: in the following, we will use the general term *p*-quinone when we refer to both the *p*-hydro- and the *p*-benzoquinone state).[1] As a consequence, the assignment of a formal oxidation number to the metal centre in hydroquinonate complexes often becomes ambiguous such that the more meaningful physical oxidation number has to be established experimentally.[14]

In our own studies, we initially employed the ditopic *p*-hydroquinone chelate ligand **A**[15] (Figure 1). Treatment of **A** with Cu^{II} ions leads to the purple-coloured coordination polymer **D**, which consists of magnetically isolated linear chains with Cu^{II} ions in a square-planar coordination environment (Figure 2).

The compound behaves as a homogeneous antiferromagnetic $S=^1/_2$ Heisenberg spin chain with a moderate antiferromagnetic exchange-coupling constant $|J|/k_B$ of 21.5 K.[16–20] Moreover, it was found that subtle changes in the substitution pattern of ligand **A** led to redox reactions with the formation of Cu^{I} ions and *p*-benzoquinones rather than to polymer formation.[21] These results not only prove the promising potential of **A** as a mediator of magnetic Cu^{II}–Cu^{II} interactions, but also suggest extensive ligand-to-metal charge transfer in its Cu^{II} complexes. In spite of such desirable properties, ligand **A** also suffers from certain disadvantages. Most importantly, the synthesis of discrete dinuclear Cu^{II} complexes of **A** turned out to be difficult mainly because of a pronounced tendency for the components to form insoluble microcrystalline precipitates.[18] Discrete complexes of *p*-hydroquinonate ligands not only serve as important soluble model compounds for notoriously insoluble coordination polymers, but they are also interesting in their own right. With the aim of having more versatile *p*-hydroquinone ligands at hand, we therefore prepared a second

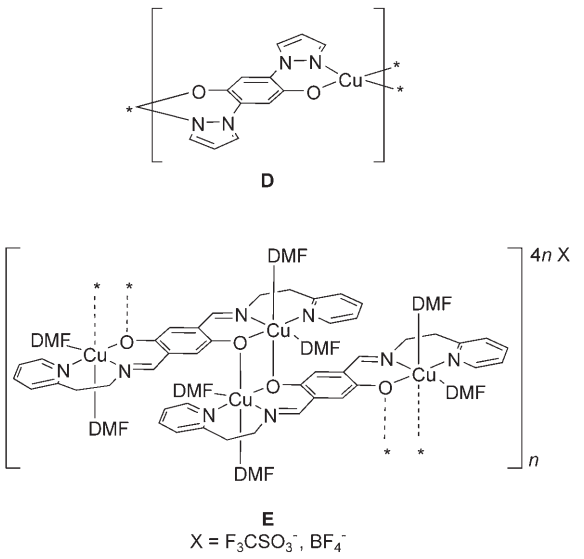

Figure 2. Heisenberg ($S=^1/_2$) spin chains **D** from ligand **A** and polymeric $S=^1/_2$ spin dimer system **E** from ligand **B**.

generation of derivatives **B** (Figure 1) equipped with bidentate tethers to occupy three coordination sites of the complexed metal ion. Depending on the steric demand of the R substituents, the new **B** ligands provided access to stable dinuclear Cu^{II} complexes (R = N*i*Pr$_2$) and to zigzag polymers **E** (R = 2-pyridyl, DMF = *N*,*N*-dimethylformamide; Figure 2).[22] Compound **E**, which behaves as an $S=^1/_2$ spin dimer system with weak three-dimensional magnetic couplings, turned out to be particularly interesting. At very low temperatures, the material undergoes a magnetic-field-induced phase transition that can be interpreted as a Bose–Einstein condensation of magnons.[22–25]

All structurally characterised complexes of **B** are either square planar or octahedral and show a meridional coordination mode of the tridentate chelator. To broaden the scope of the ligand system further, we thus decided to develop a third generation of facially coordinating *p*-hydroquinone derivatives. Given the rich chemistry of ferrocene-based poly(pyrazol-1-yl)borates, an appealing approach would be to introduce bis(pyrazol-1-yl)borate substituents at the 2- and 5-positions of the *p*-hydroquinone core. However, the preparation of these new target molecules would require extensive protective group chemistry to avoid problems that arise from the simultaneous presence of OH substituents and three-coordinate boryl groups in the key intermediates of the synthesis sequence. To circumvent these problems, we decided to switch from bis(pyrazol-1-yl)borates to bis(pyrazol-1-yl)methanes[26] and to prepare ditopic ligand **C** (Figure 1), which has the advantage of being accessible from the same starting material (2,5-diformyl-1,4-dihydroxybenzene[27]) as imine ligand **B**. Moreover, deprotonation of the OH groups during metal complexation renders each of the metal binding sites monoanionic so that they have the same charge as common poly(pyrazol-1-yl)borates.[13] Similar to boron-based scorpionate ligands, variation of the R′ sub-

stituents at the 3-positions of the pyrazolyl rings allows extensive control over the steric demand of ligand system **C**.

The range of potential applications of *p*-quinone-based bis(pyrazol-1-yl)methane ligands goes far beyond materials science. In 1997, Higgs and Carrano established (2-hydroxyphenyl)bis(pyrazol-1-yl)methanes as a new class of biomimetically relevant scorpionate ligands.[28] Because *p*-quinones have not only been recognised as ubiquitous electron-transfer agents in biology, but also as important redox cofactors ("quinoenzymes"),[29] replacement of the 2-hydroxyphenyl substituent in (2-hydroxyphenyl)bis(pyrazol-1-yl)methanes by a *p*-hydroquinone moiety as in **C** could provide interesting perspectives for modelling the active sites of *p*-hydroquinone-containing metalloenzymes, such as copper-dependent amine oxidases (cofactor: topaquinone = 2,4,5-trihydroxyphenylalaninequinone).[30–32] Further evidence for the potential of **C**-type ligands in homogeneous catalysis stems from Bäckvall et al. who employed *p*-hydroquinone as a co-catalyst in Pd^{II}-catalysed aerobic oxidations of monoolefins and conjugated dienes.[33] Moreover, Pd^{II} complexes of simple bidentate nitrogen ligands are active catalysts for styrene/CO copolymerisation provided that *p*-benzoquinone is added to the methanolic reaction mixture.[34] The role of *p*-benzoquinone lies in its ability to stabilise Pd^0 intermediates and, in the presence of acid, to reoxidise them back to Pd^{II}.[35] The Pd^{II}/*p*-benzoquinone system can also be applied to electrophilic C–H activations that can be regarded as combined Murai and Heck reactions.[36] Recently, homocoupling reactions of aryl halides have been achieved with the help of Pd^{II} catalysts that contain 1,4-diazabutadiene ligands in the presence of stoichiometric amounts of *p*-hydroquinone.[37] For a related reaction, a mechanistic model that provides an insight into the role of the *p*-hydroquinone reagent has been proposed.[38]

Thus, for applications in catalysis and materials science, mono- (e.g., **2a**–**2c**; Scheme 1) and ditopic (**4**; Scheme 1) *p*-hydroquinone-based bis(pyrazol-1-yl)methane ligands have been included in our investigations and their synthesis, reactivity and coordination behaviour will be described herein.

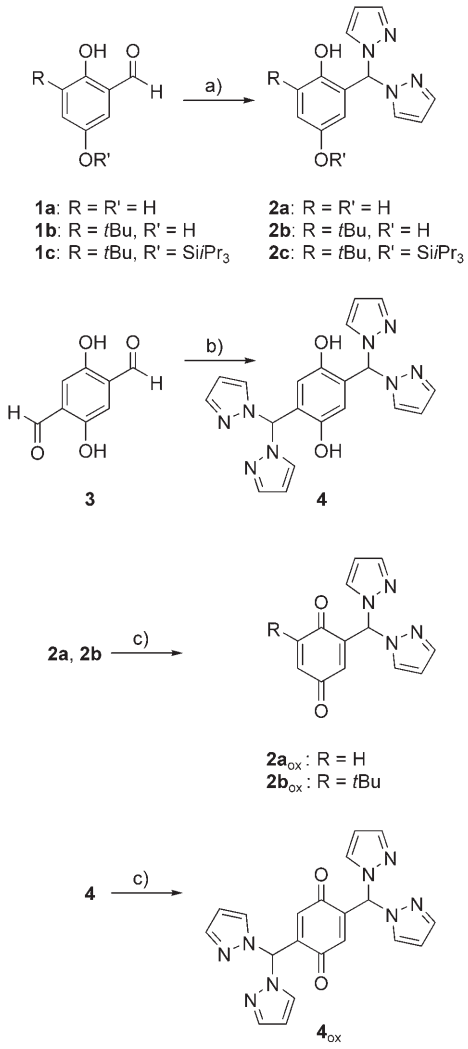

Scheme 1. Synthesis of mono- and ditopic *p*-hydroquinone-based bis(pyrazol-1-yl)methane ligands **2a**–**c**, **4** and their oxidised *p*-benzoquinone forms $\mathbf{2a}_{ox}$, $\mathbf{2b}_{ox}$ and $\mathbf{4}_{ox}$. Reagents and conditions: a) pz_2CO (1 equiv), cat. $CoCl_2$, THF, reflux; b) pz_2CO (2 equiv), cat. $CoCl_2$, THF, reflux; c) $[Ce(NH_4)_2(NO_3)_6]$ (2 equiv), CH_3CN/H_2O, 0 °C.

Results and Discussion

Synthesis and spectroscopy: In addition to parent compound **2a** (Scheme 1), we also prepared its *tert*-butyl-substituted derivative **2b** for the following reasons: 1) A *t*Bu group increases the solubility of the free ligand and its complexes. 2) Steric shielding of the metal binding site provides extra kinetic stability for the complexes and decreases the propensity of the adjacent hydroxy group to adopt a bridging position between two metal ions.[39] 3) It is important to prevent the formation of Michael adducts between the substrate amine and the ligand in its *p*-benzoquinone state by steric protection, with regard to amine oxidase model systems in particular.[40] Triisopropylsilyl derivative **2c** (Scheme 1) was synthesised to gain access to a ligand that shuttles between the *p*-hydroquinone and the *p*-semiquinone radical state (one-electron transition) rather than between the *p*-hydroquinone and the *p*-benzoquinone forms (two-electron transition).

For the preparation of **2a** to **2c**, a synthetic protocol based on that of Peterson et al.[41–43] was employed. Treatment of aldehydes **1a** to **1c** (Scheme 1) with bis(pyrazol-1-yl)methanone (1.2 equiv) in the presence of a catalytic amount of anhydrous $CoCl_2$ gave **2a** to **2c** in yields of between 23 and 36%. In a similar reaction, compound **4** was obtained from 2,5-diformyl-1,4-dihydroxybenzene (**3**) and bis(pyrazol-1-yl)methanone (2.4 equiv; Scheme 1).

Oxidation of **2a**, **2b** and **4** to $\mathbf{2a}_{ox}$, $\mathbf{2b}_{ox}$ and $\mathbf{4}_{ox}$ was conveniently achieved by using $[Ce(NH_4)_2(NO_3)_6]$ (2 equiv) in CH_3CN/H_2O (Scheme 1). In the case of $\mathbf{2b}_{ox}$ we have also successfully tested $FeCl_3$ and $NaIO_4$ as oxidising agents.

We started our assessment of the coordination properties of ligands **2** with the d^8 metal ions Ni^{II} and Pd^{II}. In the case

of Ni^{II}, octahedral complex **5** was obtained from [Ni(OAc)$_2$·4H$_2$O] and **2c** (2 equiv) in MeOH with NaOMe as the base (Scheme 2). Square-planar Pd^{II} complexes **6** and

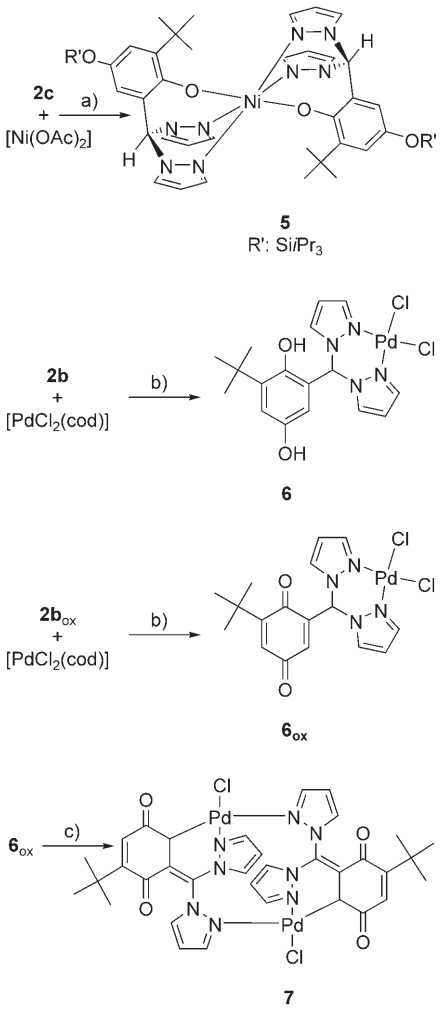

Scheme 2. Synthesis of the Ni^{II} and Pd^{II} complexes **5**, **6** and $\mathbf{6}_{ox}$. Formation of macrocyclic dinuclear Pd^{II} complex **7** by deprotonation of $\mathbf{6}_{ox}$. Reagents and conditions: a) NaOMe, MeOH, RT; b) CH_3CN, RT; c) NEt_3, CH_3CN, RT

$\mathbf{6}_{ox}$, with their redox-active substituents in the *p*-hydroquinone and *p*-benzoquinone state, respectively, were readily formed from [$PdCl_2$(cod)] and **2b**/$\mathbf{2b}_{ox}$ in CH_3CN (Scheme 2; cod: cyclooctadiene).

The electron-withdrawing effect of the two sp^2 nitrogen substituents in bis(pyrazol-1-yl)methane leads to an increase in the acidity of the methylene protons so that they can be easily abstracted by suitable bases. The considerable synthetic potential of this reaction was first exploited by Otero et al. who prepared the *N*,*N*,*O*-scorpionate ligand bis(3,5-dimethylpyrazol-1-yl)acetate by treatment of bis(3,5-dimethylpyrazol-1-yl)methane with *n*BuLi followed by the addition of CO_2.[44] We expected the methine protons in $\mathbf{2a}_{ox}$ and $\mathbf{2b}_{ox}$ to be even more acidic than the methylene protons in the parent H_2Cpz_2 because of the negative mesomeric effect of the *p*-benzoquinone substituent. To test this hypothesis, NEt_3 was added to a small quantity of the Pd^{II} complex $\mathbf{6}_{ox}$ in CH_3CN. An NMR spectroscopic investigation of the solution revealed a mixture of several products from which the remarkable dinuclear Pd^{II} macrocycle **7** could be isolated as orange single crystals (Scheme 2).

From this result it became apparent that more base-stable ligands are required for some of our further investigations and we therefore decided to replace the reactive methine proton by an inert methyl group (Scheme 3). To this end, we started from *O*-protected precursor **8** and transformed it into bis(pyrazol-1-yl)methane derivative **9** by the reaction sequence already employed for the synthesis of **2a** to **2c**. Deprotonation of **9** with *n*BuLi and subsequent methylation with MeI led to compound **10** in high yields. Deprotection

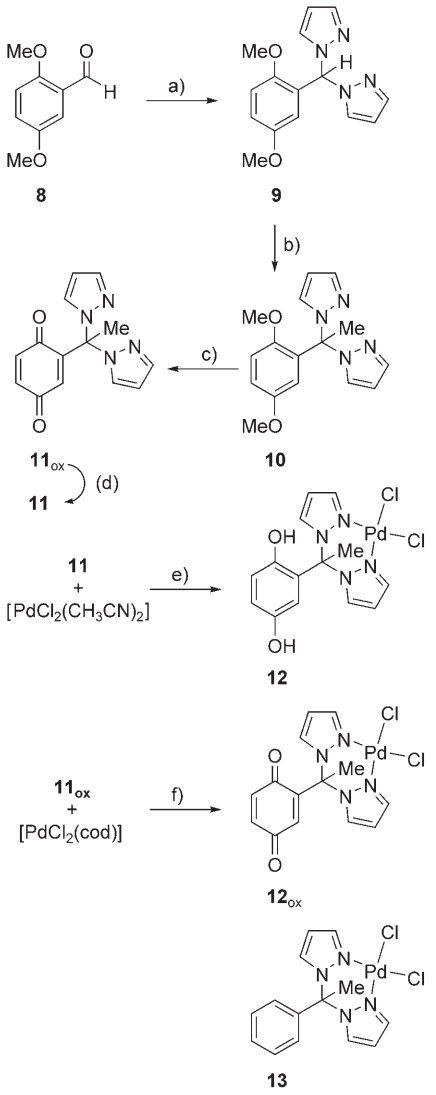

Scheme 3. Synthesis of methylated *p*-hydroquinone-based bis(pyrazol-1-yl)methane ligand **11**, its oxidised *p*-benzoquinone form $\mathbf{11}_{ox}$ and the corresponding $PdCl_2$ complexes **12** and $\mathbf{12}_{ox}$. Reagents and conditions: a) pz_2CO (1 equiv), cat. $CoCl_2$, THF, reflux; b) i) *n*BuLi (1 equiv), THF, 0 °C; ii) MeI (1 equiv), RT; c) excess [$Ce(NH_4)_2(NO_3)_6$], THF/H_2O, 0 °C; d) excess $Na_2S_2O_4$, THF/H_2O, RT; e) CH_3CN, reflux; f) CH_3CN, RT

of **10** was less straightforward. In the past, we successfully used a mixture of hydrobromic and acetic acids to generate various *p*-hydroquinone derivatives from their methoxy precursors.[27] In the special case of **10**, however, we encountered problems with the stability of the bis(pyrazol-1-yl)methane moiety in strongly acidic media. We finally developed a convenient oxidative procedure that leads to $\mathbf{11}_{ox}$ upon treatment of **10** with excess $[Ce(NH_4)_2(NO_3)_6]$ in THF/H_2O. The corresponding *p*-hydroquinone ligand **11** is readily accessible from $\mathbf{11}_{ox}$ and $Na_2S_2O_4$ as the reducing agent. Reaction of **11**/$\mathbf{11}_{ox}$ with $[PdCl_2(CH_3CN)_2]$ and $[PdCl_2(cod)]$, respectively, provided the $PdCl_2$ complexes **12**/$\mathbf{12}_{ox}$. For reasons not yet understood, the synthesis of **12** from **11** and $[PdCl_2(cod)]$ repeatedly failed even though this Pd^{II} complex was successfully employed in the preparation of the closely related complex **6** (Scheme 2).

The ^{1}H NMR spectrum of **2a** in MeOD is characterised by a singlet (integrating to 1H) at $\delta = 7.91$ ppm for the methine proton C*H*pz_2, a set of three signals ($\delta = 7.61$, 7.47 and 6.36 ppm; each integrating to 2H) for the two chemically equivalent pyrazol-1-yl substituents and two signals ($\delta = 6.73$ (2H) and 6.27 ppm (1H)) for the *p*-hydroquinone core. Upon oxidation to $\mathbf{2a}_{ox}$, the resonance of the methine proton is shifted by 0.07 ppm to a higher field ($\mathbf{2a}_{ox}$: δ(C*H*pz_2) = 7.84; MeOD). Minor differences between **2a** and $\mathbf{2a}_{ox}$ are also observed in the chemical shifts of the pyrazol-1-yl signals ($\delta = 7.78$, 7.63 and 6.41 ppm) and in the resonances of the six-membered ring ($\delta = 6.84$ (2H) and 6.19 ppm (1H)). Two of the three protons of the *p*-quinone fragments in **2a** and $\mathbf{2a}_{ox}$ are fortuitously isochronous.

The ^{13}C NMR resonances of the parent *p*-hydroquinone appear at $\delta = 150.6$ (*C*OH) and 117.0 ppm (*C*H) and those of *p*-benzoquinone at $\delta = 187.0$ (*C*O) and 136.4 ppm (*C*H).[45] Thus, the two resonances at 151.6 and 149.4 ppm in the spectrum of **2a** have to be assigned to the hydroxylated carbon atoms. The corresponding CO signals in $\mathbf{2a}_{ox}$ possess chemical shifts of $\delta = 188.3$ and 186.3 ppm. As can be expected from the comparison of the ^{13}C NMR spectra of the parent species, the remaining four resonances of the six-membered ring of **2a** are grouped around $\delta = 117$ ppm (i.e., $\delta = 123.3$, 118.8, 117.7 and 115.5 ppm), whereas the corresponding chemical shifts of $\mathbf{2a}_{ox}$ are close to $\delta = 136$ ppm (i.e., $\delta = 143.7$, 138.2, 137.9 and 135.5 ppm). The signals of the methine carbon atoms of **2a** and $\mathbf{2a}_{ox}$ are found at $\delta =$ 75.0 and 72.8 ppm, respectively. Similar to the ^{1}H NMR spectra, the ^{13}C NMR spectra of **2a** and $\mathbf{2a}_{ox}$ reveal only negligible differences in the chemical shifts of their pyrazol-1-yl signals.

In the NMR spectra of **2b** and $\mathbf{2b}_{ox}$, the signals of the *t*Bu groups are visible at $\delta(^1H) = 1.41$ (**2b**) and 1.21 ppm ($\mathbf{2b}_{ox}$) and $\delta(^{13}C) = 35.7$, 29.8 (**2b**) and 36.5, 29.8 ppm ($\mathbf{2b}_{ox}$). The NMR spectra of **2c** are characterised by additional resonances at $\delta(^1H) = 1.19$, 1.08 ppm and $\delta(^{13}C) = 17.9$, 12.6 ppm for the Si*i*Pr_3 fragment.

The NMR spectra of **4** and $\mathbf{4}_{ox}$ contain the same general features as those of **2a** and $\mathbf{2a}_{ox}$. However, the integral ratios of the proton resonances of **4** clearly indicate the presence of two $CHpz_2$ substituents in this molecule. Moreover, **4** and $\mathbf{4}_{ox}$ give rise to fewer NMR signals than **2a** and $\mathbf{2a}_{ox}$, in accordance with the higher molecular symmetry of the ditopic ligands.

Complex **5** contains a high-spin Ni^{II} centre and is therefore paramagnetic. As a result, NMR spectra obtained were not interpretable.

The NMR spectra of **6** and $\mathbf{6}_{ox}$ are rather similar to those of free ligands **2b** and $\mathbf{2b}_{ox}$. However, as a characteristic difference we note a downfield shift of the pzC-3,5 resonances upon complexation (**2b**: $\delta = 141.1$, 131.8 ppm; **6**: $\delta = 145.0$, 136.5 ppm; $\mathbf{2b}_{ox}$: $\delta = 142.2$, 131.7 ppm; $\mathbf{6}_{ox}$: $\delta = 145.7$, 137.0 ppm).

As can be expected, the NMR spectra of **11** and $\mathbf{11}_{ox}$ closely resemble those of **2a** and $\mathbf{2a}_{ox}$. In the ^{1}H NMR spectra of **11** and $\mathbf{11}_{ox}$ the characteristic low-field resonances of the methine protons are missing and signals for the C(*Me*)pz_2 methyl groups are found instead (**11**, $\mathbf{11}_{ox}$: $\delta =$ 2.67 ppm). In the ^{13}C NMR spectra, the resonances of the methyl carbon atoms C(*Me*)pz_2 appear at $\delta = 25.4$ ppm in **11** and at $\delta = 25.1$ ppm in $\mathbf{11}_{ox}$.

All relevant NMR data for **12** and $\mathbf{12}_{ox}$ are consistent with those of **6** and $\mathbf{6}_{ox}$ and therefore do not merit further discussion.

X-ray crystallography: Details of the X-ray crystal structure analyses of **5**, **6**, **7** and $\mathbf{12}_{ox}$ are summarised in Table 1. The X-ray crystal structure analyses of the free ligands **2a**, $\mathbf{2b}_{ox}$, **2c**, **4**, the intermediate **9** and complex **13** (Scheme 3) are described in the Supporting Information.

In complex **5**, two ligands **2c** bind to a Ni^{II} ion in a *trans* configuration (Figure 3). The molecule contains a centre of inversion at Ni1 together with a mirror plane that is spanned by the two *p*-hydroquinonyl moieties and the Ni^{II} ion.

The octahedral coordination sphere of Ni^{II} is largely undistorted. The angles between the *trans* positions possess a crystallographically imposed value of precisely 180.0° and the angles between the *cis* positions lie in the range of 86.5(1) (N-Ni-N chelate bite angle) to 93.5(1)° (N-Ni-N non-chelate angle). The Ni–N and Ni–O bond lengths of 2.079(1) and 2.022(1) Å, respectively, are comparable to the corresponding values in the related complex *trans*-$[NiL_2]$,[46] which features a Ni^{II} ion and two deprotonated (2-hydroxyphenyl)bis(pyrazol-1-yl)methane ligands L^- (two crystallographically independent molecules in the solid state; average values Ni–N/Ni–O: 2.088(7)/2.011(7) Å). It is thus apparent that the presence of the bulky *tert*-butyl group in **5** does not enforce significant stretching of the Ni–(N,O) bonds. Upon coordination, the O–C_{ipso} bond shortens from 1.368(1) Å in **2c** (cf. the Supporting Information) to 1.304(2) Å in **5**. In contrast, the *i*Pr_3SiO–C_{ipso} bond lengths in **2c** (1.372(1) Å) and **5** (1.385(2) Å) are roughly the same. Differences similar to those noted for **2c** and **5** have also been observed between the free ligand (2-hydroxyphenyl)-bis(pyrazol-1-yl)methane (LH: HO–C_{ipso} 1.372(7) Å[28]) and its corresponding complex $[NiL_2]$ (NiO–C_{ipso} 1.309(13) Å[46]). We attribute the shorter NiO–C_{ipso} bonds in **5** and $[NiL_2]$ to

Table 1. Crystal data and structure refinement details for **5**, **6**, **7** and $\mathbf{12}_{ox}$.

Compound	**5**	**6**	**7**	$\mathbf{12}_{ox}$
formula	$C_{52}H_{78}N_8NiO_4Si_2$	$C_{17}H_{20}Cl_2N_4O_2Pd{\cdot}0.5C_2H_3N$	$C_{34}H_{34}Cl_2N_8O_4Pd_2{\cdot}4C_2H_3N$	$C_{14}H_{12}Cl_2N_4O_2Pd{\cdot}C_2H_3N$
M_r	994.11	510.20	1066.61	486.63
colour, shape	brown, plate	yellow, plate	orange, block	orange-brown, plate
T [K]	175(2)	165(2)	173(2)	173(2)
radiation, λ [Å]	$Mo_{K\alpha}$, 0.71073	$Mo_{K\alpha}$, 0.71073	$Mo_{K\alpha}$, 0.71073	$Mo_{K\alpha}$, 0.71073
crystal system	monoclinic	triclinic	triclinic	orthorhombic
space group	*C*2/*m*	$P\bar{1}$	$P\bar{1}$	*Pbca*
a [Å]	19.046(3)	11.262(2)	9.4514(9)	14.1130(5)
b [Å]	12.5401(15)	12.6863(16)	10.8218(10)	14.7185(6)
c [Å]	14.1605(16)	15.9035(15)	12.7740(12)	18.1331(6)
α [°]	90	111.725(9)	70.762(7)	90
β [°]	90.796(11)	93.102(16)	75.746(8)	90
γ [°]	90	97.949(11)	73.388(7)	90
V [Å^3]	3381.7(7)	2076.8(5)	1165.29(19)	3766.6(2)
Z	2	4	1	8
D_{calcd} [g cm^{-3}]	0.976	1.632	1.520	1.716
F(000)	1068	1028	540	1936
μ [mm^{-1}]	0.362	1.173	0.940	1.290
crystal size [mm]	0.44×0.42×0.14	0.70×0.50×0.06	0.16×0.14×0.08	0.28×0.12×0.03
rflns collected	21 104	32 005	19 315	56 934
independent rflns (R_{int})	4973 (0.0276)	11 532 (0.0771)	4374 (0.0821)	4343 (0.0529)
data/parameters	4973/186	11 532/501	4374/283	4343/238
GOF on F^2	1.057	1.009	1.032	1.037
R_1, wR_2 [$I>2\sigma(I)$]	0.038, 0.099	0.041 , 0.095	0.065, 0.168	0.023, 0.057
R_1, wR_2 (all data)	0.048, 0.104	0.067, 0.110	0.070, 0.174	0.028, 0.058
largest diff peak and hole [e Å^{-3}]	0.38, −0.29	0.86, −1.43	1.17, −1.88	0.36, −0.56

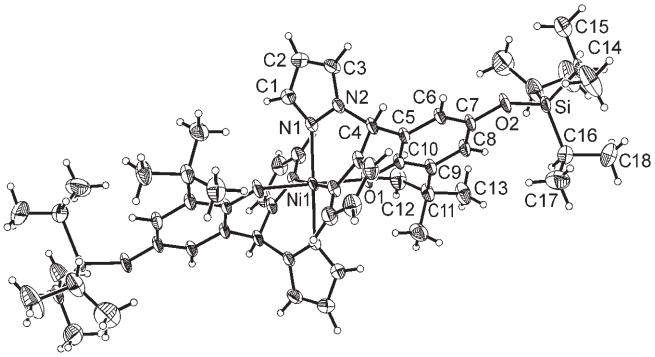

Figure 3. X-ray crystal structure of **5** (50% probability ellipsoids). Selected bond lengths [Å], bond angles [°] and torsion angles [°]: Ni1−N1 2.079(1), Ni1−O1 2.022(1), O1−C10 1.304(2), O2−C7 1.385(2), N2−C4 1.463(1), C4−C5 1.511(2); O1-Ni1-O1* 180.0, N2-C4-N2# 110.5(1), C4-C5-C6 114.5(1), C4-C5-C10 123.1(1); N1-N2-C4-C5 77.8(1). Symmetry transformations used to generate equivalent atoms: $-x,-y+1,-z+1$ (*); $x,-y+1,z$ (#).

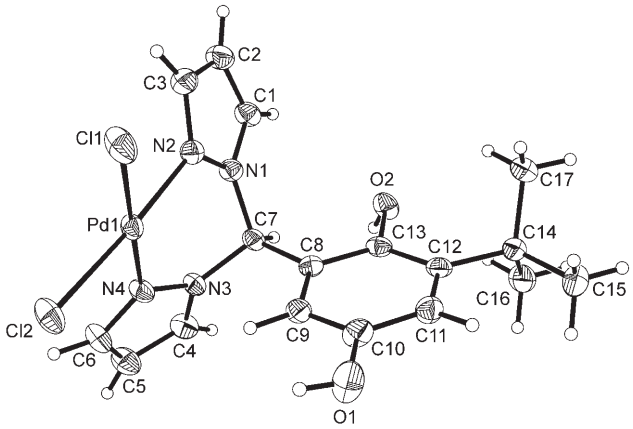

Figure 4. X-ray crystal structure of $\mathbf{6}_A$ (50% probability ellipsoids). Selected bond lengths [Å], bond angles [°], torsion angles [°] and dihedral angles [°]: Pd1−Cl1 2.283(1), Pd1−Cl2 2.295(1), Pd1−N2 2.024(3), Pd1−N4 2.020(3), O1−C10 1.368(4), O2−C13 1.396(3), N1−C7 1.456(4), N3−C7 1.461(4); Cl1-Pd1-Cl2 90.2(1), Cl1-Pd1-N2 90.5(1), Cl1-Pd1-N4 179.5(1), N2-Pd1-N4 89.3(1), N2-Pd1-Cl2 175.6(1), N4-Pd1-Cl2 90.0(1); N2-N1-C7-C8 −69.6(4), N4-N3-C7-C8 76.8(4); Cl1-Pd1-Cl2//N2-Pd1-N4 4.4, N1pz//N3pz 49.0.

a larger degree of O→Aryl π bonding, which leads to more O−C double bond character compared with the protonated free ligands.

Compound **6** crystallises from CH_3CN with two crystallographically independent molecules in the asymmetric unit ($\mathbf{6}_A$ and $\mathbf{6}_B$). Both molecules adopt a chiral conformation. Differences in the structural parameters of $\mathbf{6}_A$ and $\mathbf{6}_B$ are close to the margins of experimental error and therefore do not merit further discussion. Thus, only the molecular structure of $\mathbf{6}_A$ is considered herein (Figure 4).

The square-planar complex of $\mathbf{6}_A$ features a $PdCl_2$ moiety coordinated to the two pyrazol-1-yl rings of the ligand. All of the bond lengths and bond angles agree nicely with the values of the related compound $[PdCl_2\{Ph_2C(pz)_2\}]$[47] on the one hand and **2a** (cf. the Supporting Information) on the other. Somewhat surprisingly, the complex fragment is turned away from the HO2 hydroxy group even though a

closer approach between Pd1 and the O2 atom might have been anticipated on electrostatic grounds.

Centrosymmetric macrocycle **7** contains two Pd^{II} ions, each of them surrounded by one chloride ligand, two pyrazolyl rings and one carbon atom in a square-planar fashion (Figure 5). For the bis(pyrazol-1-yl)methyl moieties, a bridging rather than a chelating coordination mode is observed, which results in significantly different Pd–N bond lengths of 2.053(4) (Pd1–N12) and 2.139(4) Å (Pd1–N22A).

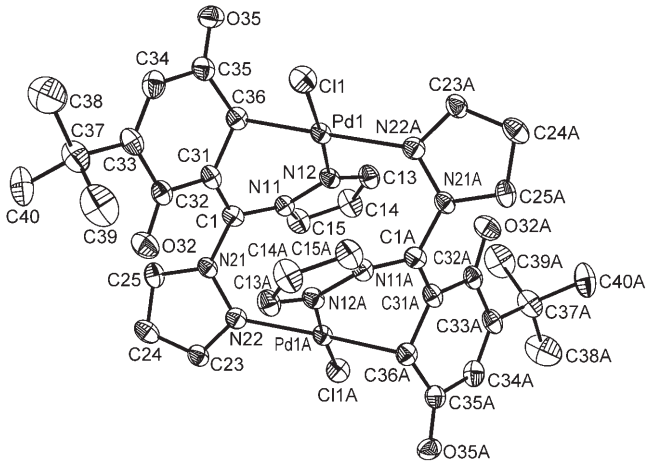

Figure 5. X-ray crystal structure of **7** (50% probability ellipsoids). Selected bond lengths [Å], bond angles [°] and torsion angles [°]: Pd1–Cl1 2.309(1), Pd1–N12 2.053(4), Pd1–N22A 2.139(4), Pd1–C36 2.082(5), N11–C1 1.417(6), N21–C1 1.414(6), C1–C31 1.351(7), O32–C32 1.225(6), O35–C35 1.225(6), C31–C32 1.504(6), C31–C36 1.469(7), C32–C33 1.513(7), C33–C34 1.336(8), C34–C35 1.489(7), C35–C36 1.490(7); Cl1-Pd1-N12 176.2(1), Cl1-Pd1-N22A 90.6(1), Cl1-Pd1-C36 94.6(1), N12-Pd1-N22A 92.5(2), N22A-Pd1-C36 173.6 (2), N12-Pd1-C36 82.4(2), Pd1-C36-C31 101.8(3), N11-C1-N21 112.9(4), N11-C1-C31 121.0(4), N21-C1-C31 126.1(4); N11-C1-C31-C32 –163.5(4), N21-C1-C31-C32 18.2(7). Symmetry transformation used to generate equivalent atoms: $-x+1,-y+1,-z+1$ (A).

The shorter Pd–N bond is part of a six-membered PdN_2C_3 palladacycle. We note that the Pd1–C36 (2.082(5) Å) bond of **7** is 0.112 Å longer than the Pd–C(sp^2) bond in [PdCl(Ph)(2,2′-bipy)] (1.970(7) Å)[48] and still 0.062 Å longer than the Pd–C(sp^3) bond in [PdCl(CH_3)(NN)] (2.020(11) Å;[49] NN: ArN=C(H)C(H)=NAr, Ar: 2,6-(iPr)$_2$C$_6$H$_3$). However, it agrees nicely with the Pd–C bond length in [PdCl(CH_2C(O)CH_3)(2,2′-bipy)] (2.084(7) Å)[50] in which the electron lone-pair at the donor carbon atom is conjugated with a carbonyl group. This situation is closely related to our macrocycle. The C31–C36 and C1–C31 distances in **7** are indicative of a shortened single bond (1.469(7) Å) and a double bond (1.351(7) Å), respectively. Moreover, the Pd1-C36-C31 bond angle of 101.8(3)° is close to the ideal tetrahedral angle (109.5°) and both sums of angles with vertices at C1 and C31 exactly match 360°. The CO bond lengths of 1.225(6) Å and the C33–C34 bond length of 1.336(8) Å are almost identical to the corresponding values in **2b**$_{ox}$ (cf. the Supporting Information). These data lead to the conclusion that treatment of **6**$_{ox}$ with NEt_3 causes deprotonation of the methine carbon atom (C1 in Figure 5) with subsequent delocalisation of the resulting electron lone-pair into the *p*-benzoquinonyl substituent. In turn, the electron density is shifted to the carbon atom *ortho* to the bis(pyrazol-1-yl)methyl fragment (C36 in Figure 5), which thereby gains sufficient nucleophilic character to bind to the Lewis acidic Pd^{II} centre.

Single crystals of **12**$_{ox}$ were grown from Et_2O/CH_3CN (Figure 6); the compound crystallises with CH_3CN (1 equiv). The molecule contains one Pd^{II} ion coordinated by two chloride ions and the bis(pyrazol-1-yl)methane fragment in a square-planar fashion.

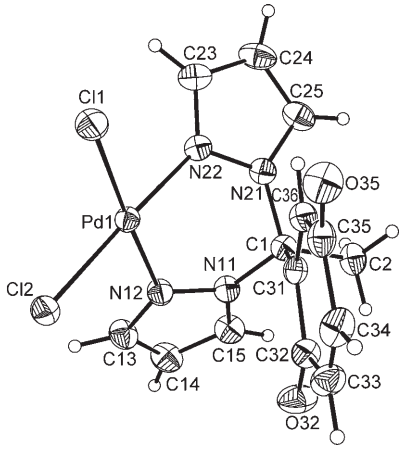

Figure 6. X-ray crystal structure of **12**$_{ox}$ (50% probability ellipsoids). Selected bond lengths [Å], bond angles [°], torsion angles [°] and dihedral angles [°]: Pd1–Cl1 2.290(1), Pd1–Cl2 2.294(1), Pd1–N12 2.024(1), Pd1–N22 2.034(2), O32–C32 1.223(2), O35–C35 1.231(2), C31–C32 1.498(2), C32–C33 1.487(3), C33–C34 1.335(3), C34–C35 1.472(3), C35–C36 1.487(2), C31–C36 1.340(2), N11–C1 1.474(2), N21–C1 1.479(2); Cl1-Pd1-Cl2 92.49(2), Cl1-Pd1-N12 177.2(1), Cl1-Pd1-N22 90.1(1), N12-Pd1-N22 87.1(1), N12-Pd1-Cl2 90.3(1), N22-Pd1-Cl2 177.3(1); N12-N11-C1-C31 53.1(2), N22-N21-C1-C31 –63.3(2); Cl1-Pd1-Cl2//N12-Pd1-N22 0.9, N11pz//N21pz 57.9.

Similar to the molecular structure of **6**, there is no short contact between the O32 atom and the Pd^{II} centre in **12**$_{ox}$. The redox-active substituent shows two short C–O bonds (average value = 1.227(2) Å) together with strongly alternating C–C bond lengths (e.g., C32–C33 1.487(3) Å, C33–C34 1.335(3) Å), which clearly proves that it is in its *p*-benzoquinone state. All of the relevant bond lengths and angles of **12**$_{ox}$ are close to the corresponding values in the free *p*-benzoquinone-based ligand **2b**$_{ox}$ (cf. the Supporting Information) and in the related Pd^{II} complex [$PdCl_2${$Ph_2C(pz)_2$}].[47]

Electrochemical investigations: Compounds **11**, **11**$_{ox}$, **12** and **12**$_{ox}$ were investigated by cyclic voltammetry (CH_3CN, [NBu_4]PF_6 (0.1 M); vs. FcH/FcH^+). For comparison, Pd^{II} complex **13** (Scheme 3), which bears a redox-inactive phenyl substituent, was synthesised (cf. the Supporting Information) and included in our investigation.

The cyclic voltammograms (CV) of **11** and **12** reveal irreversible redox transitions with peak potentials of $E_{pa} \approx 0.55$, 0.68 (**11**) and 0.63, 0.79 V (**12**), which were assigned to the *p*-hydroquinone→*p*-semiquinone→*p*-benzoquinone redox transitions (cf. Figure S7 in the Supporting Information). The chemical irreversibility most likely results from the loss of HO protons during oxidation.[51] We note that the voltammogram of **11** is qualitatively similar to that of the related *p*-hydroquinone-containing ditopic imine ligand **B** (R = N*i*Pr$_2$; Figure 1).[22] Compound **12** features an irreversible reduction wave at $E_{pc} = -1.23$ V that is also present in the CV of **13** ($E_{pc} \approx -1.30$ V; Figure S7) but absent in the voltammogram of **11**. We therefore assign this redox event to a palladium-centred electron transition.

p-Benzoquinone species **11**$_{ox}$ and **12**$_{ox}$ are electrochemically better behaved than their *p*-hydroquinone congeners. CVs of **11**$_{ox}$, **12**$_{ox}$ and **13** are juxtaposed in Figure 7.

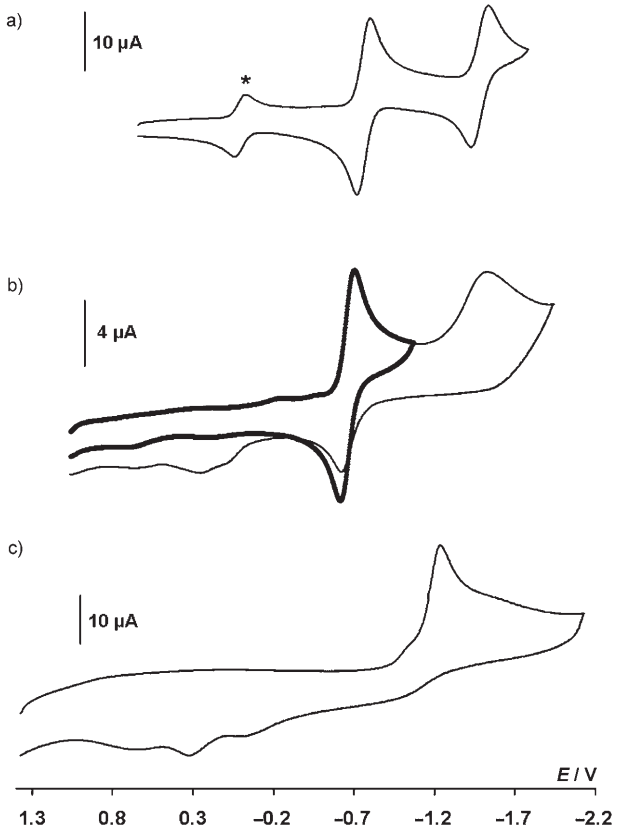

Figure 7. Cyclic voltammograms of a) **11**$_{ox}$, b) **12**$_{ox}$ and c) **13**. CH_3CN solutions, $[NBu_4]PF_6$ (0.1 M), scan rates: a) 100 mV s^{-1}, b and c) 200 mV s^{-1}, vs. FcH/FcH$^+$ (*).

Free ligand **11**$_{ox}$ gives rise to two redox waves with features that indicate electrochemical reversibility: the current ratios (i_{pc}/i_{pa}) are constantly equal to one, the current functions $i_{pa}/v^{1/2}$ remain constant and the peak-to-peak separations (ΔE) do not deviate appreciably from the value found for the internal ferrocene standard (ΔE(FcH); theoretically expected value for a chemically and electrochemically reversible one-electron step: $\Delta E = 59$ mV). The first one-electron reduction of **11**$_{ox}$ to [**11**$_{ox}$]$^{\bullet-}$ occurs at a potential of $E_{1/2} = -0.79$ V ($\Delta E = 85$ mV); for the second reduction step to [**11**$_{ox}$]$^{2-}$, a potential of $E_{1/2} = -1.53$ V ($\Delta E = 110$ mV) was determined. The peak current associated with the second electron transfer is somewhat smaller than the peak current of the first transition. This phenomenon has already been described in the literature for other *p*-benzoquinone derivatives.[52,53] The CV of the Pd^{II} complex **12**$_{ox}$ recorded up to a potential of $E = -1.2$ V (bold line in Figure 7b) exhibits a chemically reversible redox wave at a potential of $E_{1/2} = -0.69$ V ($\Delta E = 79$ mV) that agrees nicely with the first redox event of **11**$_{ox}$. When the sweep is continued into the cathodic regime, a broad and irreversible wave is detected at $E_{pc} \approx -1.58$ V. Moreover, the anodic current of the first redox event decreases significantly in the reverse scan and new, ill-defined features appear in the potential range between 0 and 0.5 V (Figure 7). Similar features are apparent in the CV of complex **13**, together with an irreversible wave at $E_{pc} \approx -1.30$ V. The CVs of **11**$_{ox}$ and **13** indicate that *p*-semiquinonate and Pd^{II} reduction require comparable electrode potentials. As a consequence, it cannot be safely concluded whether the broad cathodic wave of **12**$_{ox}$ can be assigned to a ligand- or metal-centred redox transition or whether both occur simultaneously.

Exploratory reactivity studies: As already mentioned in the Introduction, Pd^{II}/1,4-diazabutadiene complexes in the presence of *p*-hydroquinone have been successfully used in the Ullmann-type homocoupling of aryl halides (typical reaction conditions: K_2CO_3, $[NBu_4]Br$, DMF, 135 °C, 24 h).[37] Thus, we chose this conversion to assess the reactivity of our new complexes. As preliminary tests on the base stability of **6**/**6**$_{ox}$ have revealed the ready abstraction of the methine proton with formation of macrocyclic dimer **7** (Scheme 2), we employed methyl derivative **12** (Scheme 3) in our investigation. Treatment of **12** with a stoichiometric amount of iodobenzene (Cs_2CO_3, DMF, 150 °C, 5 h) led to the quantitative consumption of the substrate with the concomitant formation of biphenyl and benzene (NMR spectroscopic and HPLC control). Although biphenyl is the expected product, the mechanism of benzene formation is not yet understood. Nevertheless, our results can best be explained if we assume an oxidative addition of iodobenzene at the palladium centre preceded by the intramolecular electron-transfer reaction *p*-hydroquinone/Pd^{II}→*p*-benzoquinone/Pd^0.

Conclusion

Our group is interested in the development of novel redox-active ligands both for the generation of metal-containing polymers and for use in homogeneous catalysis. To this end, we have prepared a series of *p*-hydroquinone-substituted bis(pyrazol-1-yl)methane ligands (**2a**, **2b**, **2c** and **11**) and shown that the Pd^{II} complex of even the sterically least shielded derivative (**11**) is perfectly stable as a monomeric

species in solution. This is in contrast, for example, to the related chelate ligand 2-(pz)$C_6H_3(OH)_2$, which tends to give insoluble coordination polymers with various metal ions.[18] Electrochemical investigations and chemical oxidations on a preparative scale clearly reveal that free *p*-hydroquinone ligands **2a** and **2b** as well as the Pd^{II} complex [Pd**2b**Cl_2] undergo reversible electron transfer to their *p*-benzoquinone state (**2a**$_{ox}$, **2b**$_{ox}$, [Pd**2b**$_{ox}Cl_2$]). This is an important proof-of-principle of our concept given the fact that we want the *p*-quinone substituent to aid the redox chemistry of the complexed metal ion by acting as a two-electron reservoir. Problems, however, can result from the high acidity of the methine proton especially when the ligands are in their *p*-benzoquinone state. Thus, we also prepared a derivative of **2a**/**2a**$_{ox}$ in which the methine proton is replaced by a methyl group and which turned out to be perfectly base-stable. The corresponding $PdCl_2$ complex of the methylated ligand is active in the transformation of iodobenzene into biphenyl and benzene. The chemistry described in this paper is not restricted to monotopic ligands. The ditopic *p*-quinone-bridged bis(pyrazol-1-yl)methane ligands **4** and **4**$_{ox}$ are also accessible in good yields and we are currently exploring the scope of **4** and **4**$_{ox}$ as facially coordinating linkers for coordination polymer synthesis.

Experimental Section

General: All reactions and manipulations of air-sensitive compounds were carried out in dry, oxygen-free nitrogen by using standard Schlenk ware. THF was freshly distilled under argon from Na/benzophenone and CH_3CN was stored over 4 Å molecular sieves prior to use. NMR spectra were recorded with Bruker AM-250, Bruker Avance-300 and Bruker Avance-400 spectrometers. All NMR spectra were recorded at 27 °C. Abbreviations: s = singlet; d = doublet; t = triplet; vt = virtual triplet; dd = doublet of doublets; br = signal broadened; m = multiplet; n.r. = multiplet expected in the ^{1}H NMR spectrum, but not resolved; n.o. = signal not observed; pz = pyrazol-1-yl; HQ = *p*-hydroquinone core; BQ = *p*-benzoquinone core. Elemental analyses were performed by the Microanalytical Laboratory of the University of Frankfurt and by Quantitative Technologies Inc. (QTI). Mass spectra were recorded with a VG PLATFORM II-mass spectrometer. Compounds **1a** and **8** are commercially available. Compounds **1b**,[54] **1c**,[54] **3**[27] and bis(pyrazol-1-yl)methanone[42] were synthesised according to literature procedures.

Synthesis of 2a to 2c: A solution of the corresponding aldehyde (7.80 mmol) in THF (100 mL) was treated with bis(pyrazol-1-yl)methanone (1.508 g, 9.30 mmol) and anhydrous $CoCl_2$ (0.325 g, 2.50 mmol). The resulting suspension was heated at reflux for 24 h and then allowed to cool to room temperature. H_2O (50 mL) was added and the mixture stirred for an additional 30 min. The product was extracted into CH_2Cl_2 (3 × 50 mL), the combined organic phases were dried ($MgSO_4$), filtered and the filtrate was evaporated to dryness in vacuo. Flash column chromatography yielded pure products **2a** (0.720 g, 36 %), **2b** (0.682 g, 28 %) and **2c** (0.841 g, 23 %). Single crystals of **2a** were grown from hexane/MeOH (1:1) at 5 °C.

2a: R_f = 0.52 (silica gel; EtOAc/hexane/MeOH 1:1:1); ^{1}H NMR (250.1 MHz, MeOD): δ = 7.91 (s, 1H; $CHpz_2$), 7.61, 7.47 (2 × m, 2 × 2H; pzH-3,5), 6.73 (m, 2H; HQH-5,6), 6.36 (vt, 2H; pzH-4), 6.27 ppm (m, 1H; HQH-3); ^{13}C NMR (62.9 MHz, MeOD): δ = 151.6, 149.4 (HQC-1,4), 141.7, 131.3 (pzC-3,5), 123.3 (HQC-2), 118.8, 117.7 (HQC-5,6), 115.5 (HQC-3), 107.3 (pzC-4), 75.0 ppm ($CHpz_2$); LR-MS (ESI$^+$): *m*/*z* (%): 257 (25) [M^+ + H], 189 (100) [M^+ − pz]; elemental analysis calcd (%) for $C_{13}H_{12}N_4O_2 \cdot 0.5H_2O$ (256.27 + 9.01): C 58.86, H 4.94, N 21.12; found: C 58.75, H 4.56, N 20.71.

2b: R_f = 0.52 (silica gel; Et_2O/hexane 1:1); ^{1}H NMR (250.1 MHz, $CDCl_3$): δ = 10.87 (s, 1H; OH), 7.79, 7.57 (2 × m, 2 × 2H; pzH-3,5), 7.21 (s, 1H; $CHpz_2$), 6.92, 6.68 (2 × d, ^4J(H,H) = 2.9 Hz, 2 × 1H; HQH-3,5), 6.28 (vt, 2H; pzH-4), 1.41 ppm (s, 9H; $C(CH_3)_3$), n.o. (OH); ^{13}C NMR (62.9 MHz, CD_3CN): δ = 150.6, 148.0, 142.6 (HQC-1,4,6), 141.1, 131.8 (pzC-3,5), 124.2 (HQC-2), 117.5, 115.9 (HQC-3,5), 106.8 (pzC-4), 78.7 ($CHpz_2$), 35.7 ($C(CH_3)_3$), 29.8 ppm ($C(CH_3)_3$); LR-MS (ESI$^+$): *m*/*z* (%): 313 (15) [M^+ + H], 245 (100) [M^+ − pz]; elemental analysis calcd (%) for $C_{17}H_{20}N_4O_2 \cdot 0.5H_2O$ (312.37 + 9.01): C 63.53, H 6.59, N 17.42; found: C 63.00, H 6.91, N 17.57.

2c: R_f = 0.61 (silica gel; Et_2O/hexane 1:1); ^{1}H NMR (250.1 MHz, $CDCl_3$): δ = 10.88 (s, 1H; OH), 7.78, 7.58 (2 × m, 2 × 2H; pzH-3,5), 7.22 (s, 1H; $CHpz_2$), 6.99, 6.69 (2 × d, ^4J(H,H) = 2.9 Hz, 2 × 1H; HQH-3,5), 6.29 (m, 2H; pzH-4), 1.44 (s, 9H; $C(CH_3)_3$), 1.19 (m, 3H; $CH(CH_3)_2$), 1.08 ppm (m, 18H; $CH(CH_3)_2$), n.o. (OH); ^{13}C NMR (62.9 MHz, $CDCl_3$): δ = 148.5, 148.3, 141.6, 140.5 (HQC-1,4,6; pzC-3 or pzC-5), 130.7 (pzC-5 or pzC-3), 121.8, 121.2, 119.6 (HQC-2,3,5), 106.1 (pzC-4), 79.3 ($CHpz_2$), 35.2 ($C(CH_3)_3$), 29.6 ($C(CH_3)_3$), 17.9 ($CH(CH_3)_2$), 12.6 ppm ($CH(CH_3)_2$); LR-MS (ESI$^+$): *m*/*z* (%): 469 (17) [M^+ + H], 401 (100) [M^+ − pz]; elemental analysis calcd (%) for $C_{26}H_{40}N_4O_2Si$ (468.71): C 66.63, H 8.60, N 11.95; found: C 65.65, H 8.50, N 11.76.

Synthesis of 4: A solution of **3** (0.498 g, 3.00 mmol) in THF (80 mL) was treated with bis(pyrazol-1-yl)methanone (1.151 g, 7.10 mmol) and anhydrous $CoCl_2$ (0.156 g, 1.20 mmol). The resulting suspension was heated at reflux for 24 h and then allowed to cool to room temperature. H_2O (50 mL) was added and stirring was continued for another 30 min. The product was extracted into CH_2Cl_2 (3 × 50 mL), the combined organic phases were dried ($MgSO_4$), filtered and the filtrate evaporated to dryness in vacuo to yield **4** as a pale yellow solid (0.340 g, 28 %). Single crystals of **4**·DMF_2 formed upon gas-phase diffusion of Et_2O into a saturated solution of **4** in DMF. ^{1}H NMR (250.1 MHz, [D$_7$]DMF): δ = 9.82 (s, 2H; OH), 8.00 (s, 2H; $CHpz_2$), 7.75, 7.58 (2 × m, 2 × 4H; pzH-3,5), 6.69 (s, 2H; HQH-3,3′), 6.32 ppm (m, 4H; pzH-4); ^{13}C NMR (62.9 MHz, [D$_7$]DMF): δ = 147.8 (HQC-1,1′), 140.0, 129.9 (pzC-3,5), 124.6 (HQC-2,2′), 115.2 (HQC-3,3′), 105.7 (pzC-4), 72.9 ppm ($CHpz_2$); LR-MS (ESI$^+$): *m*/*z* (%): 403 (21) [M^+ + H], 335 (62) [M^+ − pz]; elemental analysis calcd (%) for $C_{20}H_{18}N_8O_2 \cdot 2C_3H_7NO$ (402.48 + 146.14): C 56.92, H 5.88, N 25.52; found: C 56.17, H 5.85, N 25.12.

Synthesis of 2a$_{ox}$, 2b$_{ox}$ and 4$_{ox}$: A solution of the appropriate *p*-hydroquinone derivative (**2a** (0.051 g, 0.20 mmol), **2b** (0.051 g, 0.16 mmol), **4** (0.081 g, 0.20 mmol)) in CH_3CN (20 mL) was treated with [$Ce(NH_4)_2(NO_3)_6$] (0.219 g, 0.40 mmol) in H_2O (20 mL) at 0 °C. The mixture was warmed to room temperature and stirred for 3 h. The respective product was extracted into EtOAc (3 × 20 mL) and the combined organic phases dried ($MgSO_4$) and filtered. The filtrate was evaporated to dryness in vacuo to give **2a**$_{ox}$ as an orange solid (0.048 g, 95 %), **2b**$_{ox}$ as a yellow solid (0.047 g, 95 %) and **4**$_{ox}$ as a yellow oil (0.076 g, 95 %). Single crystals of **2b**$_{ox}$ were grown from CH_2Cl_2/Et_2O (2:1) at 5 °C.

2a$_{ox}$: ^{1}H NMR (250.1 MHz, MeOD): δ = 7.84 (s, 1H; $CHpz_2$), 7.78, 7.63 (m, n.r., 2 × 2H; pzH-3,5), 6.84 (m, 2H; BQH-5,6), 6.41 (n.r., 2H; pzH-4), 6.19 ppm (s, 1H; BQH-3); ^{13}C NMR (62.9 MHz, MeOD): δ = 188.3, 186.3 (BQC-1,4), 143.7 (BQC-2), 142.4 (pzC-3 or pzC-5), 138.2, 137.9, 135.5 (BQC-3,5,6), 132.1 (pzC-5 or pzC-3), 108.3 (pzC-4), 72.8 ppm ($CHpz_2$); elemental analysis calcd (%) for $C_{13}H_{10}N_4O_2$ (254.25): C 61.41, H 3.96, N 22.04; found: C 60.94, H 3.90, N 21.88.

2b$_{ox}$: ^{1}H NMR (400.1 MHz, CD_3CN): δ = 7.71 (m, 3H; $CHpz_2$, pzH-3 or pzH-5), 7.56 (m, 2H; pzH-5 or pzH-3), 6.62 (d, ^4J(H,H) = 2.4 Hz, 1H; BQH-5), 6.35 (vt, 2H; pzH-4), 6.09 (dd, ^4J(H,H) = 1.6 Hz, 2.4 Hz, 1H; BQH-3), 1.21 ppm (s, 9H; $C(CH_3)_3$); ^{13}C NMR (100.6 MHz, CD_3CN): δ = 188.9, 187.0 (BQC-1,4), 157.7, 145.9 (BQC-2,6), 142.2 (pzC-3 or pzC-5), 134.3, 133.3 (BQC-3,5), 131.7 (pzC-5 or pzC-3), 108.3 (pzC-4), 72.3 ($CHpz_2$), 36.5 ($C(CH_3)_3$), 29.8 ppm ($C(CH_3)_3$); LR-MS (ESI$^+$): *m*/*z* (%): 243 (100) [M^+ − pz]; elemental analysis calcd (%) for $C_{17}H_{18}N_4O_2$ (310.35): C 65.79, H 5.85, N 18.05; found: C 65.35, H 5.91, N 17.79.

4$_{ox}$: ^{1}H NMR (250.1 MHz, [D$_7$]DMF): δ = 8.06 (m, 4H; pzH-3 or pzH-5), 8.01 (s, 2H; $CHpz_2$), 7.64 (n.r., 4H; pzH-5 or pzH-3), 6.41 ppm (n.r., 6H;

BQH-3,3′, pzH-4); ^{13}C NMR (62.9 MHz, [D$_7$]DMF): δ = 185.1 (BQC-1,1′), 143.3 (BQC-2,2′), 141.1 (pzC-3 or pzC-5), 134.8 (BQC-3,3′), 131.2 (pzC-5 or pzC-3), 107.0 (pzC-4), 71.2 ppm (CHpz$_2$); LR-MS (ESI$^+$): *m*/*z* (%): 401 (100) [*M*$^+$+H], 333 (17) [*M*$^+$−pz]; elemental analysis calcd (%) for $C_{20}H_{16}N_8O_2$ (400.39): C 59.99, H 4.03, N 27.99; found: C 59.48, H 4.03, N 27.50.

Synthesis of 5: A solution of **2c** (0.189 g, 0.40 mmol) in MeOH (15 mL) was treated with a solution of NaOMe in MeOH (1 mL, 0.5 M). After the addition of [Ni(OAc)$_2$·4H$_2$O] (0.055 g, 0.22 mmol), the reaction mixture was stirred for 12 h at room temperature. All of the volatiles were removed in vacuo to give **5** as a pale-red solid (0.302 g, 76%). Single crystals of **5** grew upon storage of a solution in CH_2Cl_2 at −20 °C. LR-MS (ESI$^+$): *m*/*z* (%): 994 (100) [*M*$^+$+H]; elemental analysis calcd (%) for $C_{52}H_{78}N_8NiO_4Si_2$ (994.11): C 62.83, H 7.91, N 11.27; found: C 62.33, H 7.74, N 11.28.

Synthesis of 6: Neat [PdCl$_2$(cod)] (0.137 g, 0.48 mmol) was added to a solution of **2b** (0.150 g, 0.48 mmol) in CH_3CN (30 mL). The resulting yellow solution was stirred for 12 h at room temperature. All of the volatiles were removed in vacuo and the solid residue was redissolved in a minimum amount of CH_2Cl_2. Hexane was added to the solution to precipitate **6** as a yellow solid (0.20 g, 85%). Single crystals of **6** were obtained upon slow evaporation of a solution in CH_3CN. ^{1}H NMR (250.1 MHz, CD_3CN): δ = 8.13 (m, 2H; pzH-3 or pzH-5), 8.10 (s, 1H; CHpz$_2$), 8.02 (m, 2H; pzH-5 or pzH-3), 6.99 (d, ^4J(H,H) = 3.0 Hz, 1H; HQH-3 or HQH-5), 6.90 (s, 1H; OH), 6.80 (d, ^4J(H,H) = 3.0 Hz, 1H; HQH-5 or HQH-3), 6.50 (m, 2H; pzH-4), 5.60 (s, 1H; OH), 1.36 ppm (s, 9H; C(CH$_3$)$_3$); ^{13}C NMR (75.5 MHz, CD_3CN): δ = 152.2, 146.1 (HQC-1,4), 145.0 (pzC-3 or pzC-5), 142.6 (HQC-6), 136.5 (pzC-5 or pzC-3), 125.8 (HQC-2), 117.8, 113.4 (HQC-3,5), 107.9 (pzC-4), 73.4 (CHpz$_2$), 35.2 (*C*(CH$_3$)$_3$), 30.2 ppm (C(*C*H$_3$)$_2$); LR-MS (ESI$^-$): *m*/*z* (%): 489 (60) [*M*$^-$−H], 525 (100) [*M*$^-$+Cl]; elemental analysis calcd (%) for $C_{17}H_{20}Cl_2N_4O_2Pd{\cdot}H_2O$ (489.69 + 18.02): C 40.22, H 4.37, N 11.03; found: C 40.32, H 4.50, N 10.74.

Synthesis of 6$_{ox}$: Neat [PdCl$_2$(cod)] (0.048 g, 0.17 mmol) was added to a solution of **2b**$_{ox}$ (0.053 g, 0.17 mmol) in CH_3CN (15 mL). The resulting yellow solution was stirred for 12 h at room temperature, the solvent was removed in vacuo and the residue dissolved in a minimum amount of CH_2Cl_2. Hexane was added to precipitate a yellow solid of **6**$_{ox}$ that was isolated by filtration (0.060 g, 71%). ^{1}H NMR (250.1 MHz, CD_3CN): δ = 8.15, 8.10 (2×m, 2×2H; pzH-3,5), 8.00 (n.r., 1H; CHpz$_2$), 6.74, 6.65 (d, m, ^4J(H,H) = 2.4 Hz, 2×1H; BQH-3,5), 6.55 (vt, 2H; pzH-4), 1.20 ppm (s, 9H; C(CH$_3$)$_3$); ^{13}C NMR (75.5 MHz, CD_3CN): δ = 187.5, 186.1 (BQC-1,4), 157.4 (BQC-2 or BQC-6), 145.7 (pzC-3 or pzC-5), 142.7 (BQC-6 or BQC-2), 137.0 (pzC-5 or pzC-3), 135.0, 133.0 (BQC-3,5), 108.6 (pzC-4), 71.0 (CHpz$_2$), 36.1 (*C*(CH$_3$)$_3$), 29.1 ppm (C(*C*H$_3$)$_3$); LR-MS (ESI$^-$): *m*/*z* (%): 487 (100) [*M*$^-$−H]; elemental analysis calcd (%) for $C_{17}H_{18}Cl_2N_4O_2Pd{\cdot}H_2O$ (487.66 + 18.02): C 40.38, H 3.99, N 11.07; found: C 40.64, H 3.69, N 11.11.

Synthesis of 7: NEt$_3$ (0.010 g, 0.10 mmol) was added to a solution of **6**$_{ox}$ (0.020 g, 0.04 mmol) in CH_3CN (5 mL). After stirring for 12 h at room temperature, the mixture was treated with EtOAc (5 mL), washed with brine and the organic phase was separated and dried (MgSO$_4$). All of the volatiles were removed in vacuo and the greenish-brown residue was dissolved in CH_3CN (1 mL). After several days, a few orange crystals formed that were suitable for X-ray structure analysis.

Synthesis of 9: Compound **9** was synthesised in a similar manner to **2a**–**2c** from **8** (3.390 g, 20.40 mmol) and bis(pyrazol-1-yl)methanone (3.308 g, 20.40 mmol) by using a catalytic amount of anhydrous $CoCl_2$ (0.010 g, 0.08 mmol). Yield: 4.524 g (78%); R_f = 0.43 (silica gel, EtOAc/hexane, 1:1). Single crystals of **9** formed from a concentrated solution in $CHCl_3$ at room temperature. ^{1}H NMR (300.0 MHz, $CDCl_3$): δ = 7.97 (s, 1H; CHpz$_2$), 7.62, 7.41 (2×m, 2×2H; pzH-3,5), 6.88 (m, 2H; HQH-5,6), 6.49 (m, 1H; HQH-3), 6.30 (m, 2H; pzH-4), 3.71, 3.68 ppm (2×s, 2×3H; OMe); ^{13}C NMR (75.5 MHz, $CDCl_3$): δ = 153.8, 151.0 (HQC-1,4), 140.8, 129.6 (pzC-3,5), 125.3 (HQC-2), 115.4 (HQC-5 or HQC-6), 114.4 (HQC-3), 112.3 (HQC-6 or HQC-5), 106.2 (pzC-4), 73.2 (CHpz$_2$), 56.4, 55.8 ppm (OMe); LR-MS (ESI$^+$): *m*/*z* (%): 217 (100) [*M*$^+$−pz]; elemental analysis calcd (%) for $C_{15}H_{16}N_4O_2$ (284.32): C 63.37, H 5.67, N 19.70; found: C 63.35, H 5.81, N 19.84.

Synthesis of 10: A solution of *n*BuLi in hexane (2.1 M, 1.3 mL, 2.80 mmol) was added dropwise with stirring to a solution of **9** (0.800 g, 2.81 mmol) in THF (40 mL) at 0 °C. After 30 min, the resulting dark-yellow solution was allowed to warm to room temperature. Neat MeI (0.397 g, 2.80 mmol) was added and the reaction mixture was stirred for another 30 min. Water (100 mL) was added and **10** was extracted into CH_2Cl_2 (3×50 mL). The combined organic phases were dried over MgSO$_4$. Filtration and evaporation of the solvent in vacuo gave a yellow oil. The pure product of **10** (0.620 g, 74%) was obtained as a colourless oil after flash column chromatography (R_f = 0.23; silica gel; EtOAc/hexane 1:2). ^{1}H NMR (250.1 MHz, $CDCl_3$): δ = 7.63, 7.25 (2×m, 2×2H; pzH-3,5), 6.85 (m, 2H; HQH-5,6), 6.29 (m, 2H; pzH-4), 5.42 (m, 1H; HQH-3), 3.59, 3.58 (2×s, 2×3H; OMe), 2.78 ppm (s, 3H; Me); ^{13}C NMR (75.5 MHz, $CDCl_3$): δ = 153.7, 150.7 (HQC-1,4), 139.9 (pzC-3 or pzC-5), 131.8 (HQC-2), 129.3 (pzC-5 or pzC-3), 114.7, 114.0, 113.3 (HQC-3,5,6), 106.0 (pzC-4), 81.9 (*C*Mepz$_2$), 56.2, 55.5 (OMe), 25.2 ppm (Me); LR-MS (ESI$^+$): *m*/*z* (%): 231 (100) [*M*$^+$−pz]; elemental analysis calcd (%) for $C_{16}H_{18}N_4O_2$ (298.34): C 64.41, H 6.08, N 18.77; found: C 64.22, H 6.27, N 18.87.

Synthesis of 11$_{ox}$: A solution of [Ce(NH$_4$)$_2$(NO$_3$)$_6$] (9.922 g, 18.10 mmol) in H_2O (50 mL) was added with stirring at 0 °C to a solution of **10** (1.800 g, 6.03 mmol) in THF (100 mL). The reaction mixture was allowed to warm to room temperature and stirred for 3 h. Compound **11**$_{ox}$ was extracted into CH_2Cl_2 (3×50 mL), the extract was dried (MgSO$_4$), filtered and the filtrate evaporated to dryness in vacuo. The crude product of **11**$_{ox}$ (1.050 g, 65%) was purified by flash column chromatography (R_f = 0.68; silica gel; EtOAc/hexane 2:1; still contaminated with ca. 15% of **10**). ^{1}H NMR (250.1 MHz, $CDCl_3$): δ = 7.59, 7.36 (2×m, 2×2H; pzH-3,5), 6.71 (m, 2H; BQH-5,6), 6.35 (m, 2H; pzH-4), 5.45 (m, 1H; BQH-3), 2.67 ppm (s, 3H; Me); ^{13}C NMR (62.9 MHz, $CDCl_3$): δ = 187.2, 184.8 (BQC-1,4), 148.1 (BQC-2), 140.3 (pzC-3 or pzC-5), 137.6, 136.0, 132.6 (BQC-3,5,6), 128.4 (pzC-5 or pzC-3), 107.4 (pzC-4), 79.7 (*C*Mepz$_2$), 25.1 ppm (Me); LR-MS (ESI$^+$): *m*/*z* (%): 269 (82) [*M*$^+$+H], 201 (84) [*M*$^+$−pz]; elemental analysis was not obtained because even after HPLC purification **11**$_{ox}$ was still contaminated by small amounts of **10.**

Synthesis of 11: A solution of technical grade $Na_2S_2O_4$ (4.000 g, 22.97 mmol) in H_2O (40 mL) was added dropwise with stirring at room temperature to a solution of **11**$_{ox}$ (1.050 g, 3.91 mmol) in THF (60 mL). After 2 h of vigorous stirring, the reaction mixture was extracted with CH_2Cl_2 (3×50 mL) and the combined organic phases were dried (MgSO$_4$) and filtered. The filtrate was evaporated to dryness in vacuo and the solid residue was dissolved in a minimum amount of hexane/EtOAc (1:2). The solution was stored at 5 °C for several hours whereupon a colourless precipitate of **11** formed that was isolated by filtration and washed with a sparse amount of $CHCl_3$ (0.549 g, 52%). ^{1}H NMR (300.0 MHz, CD_3CN): δ = 7.57, 7.28 (2×m, 2×2H; pzH-3,5), 7.03 (br, 1H; OH), 6.70 (m, 2H; HQH-5,6), 6.50 (br, 1H; OH), 6.31 (m, 2H; pzH-4), 5.33 (dd, ^4J(H,H) = 2.7 Hz, ^5J(H,H) = 0.6 Hz, 1H; HQH-3), 2.67 (s, 3H; Me); ^{13}C NMR (75.5 MHz, CD_3CN): δ = 151.0, 148.0 (HQC-1,4), 140.5, 130.5 (pzC-3,5), 130.0 (HQC-2), 118.8, 117.6, 115.2 (HQC-3,5,6), 106.7 (pzC-4), 82.6 (*C*Mepz$_2$), 25.4 (Me); LR-MS (ESI$^+$): *m*/*z* (%): 293 (100) [*M*$^+$+Na]; elemental analysis calcd (%) for $C_{14}H_{14}N_4O_2$ (270.29): C 62.21, H 5.22, N 20.72; found: C 61.92, H 5.41, N 20.60.

Synthesis of 12: Neat [PdCl$_2$(CH$_3$CN)$_2$] (0.144 g, 0.56 mmol) was added at room temperature to a solution of **11** (0.150 g, 0.56 mmmol) in CH_3CN (25 mL). The resulting mixture was heated at reflux for 6 h. After cooling to room temperature, the solvent was removed in vacuo. The yellow residue of **12** was first washed with a mixture of CH_3CN (2 mL)/$CHCl_3$ (5 mL) and subsequently with hexane (10 mL) to give the final product (0.205 g, 82%). ^{1}H NMR (300.0 MHz, CD_3CN): δ = 8.19, 8.02 (2×br, 2×2H; pzH-3,5), 6.82, 6.76 (2×m, 2×1H; HQH-5,6), 6.75 (s, 1H; OH), 6.63 (s, 1H; OH), 6.52 (br, 2H; pzH-4), 5.49 (n.r., 1H; HQH-3), 2.66 ppm (s, 3H; Me); ^{13}C NMR (75.5 MHz, CD_3CN/[D$_6$]DMSO, 50:1): δ = 151.2, 148.3 (HQC-1,4), 144.9, 134.3 (2×br, pzC-3,5), 127.5 (HQC-2), 118.9, 118.8 (HQC-5,6), 115.1 (HQC-3), 107.4 (br, pzC-4), 82.0 (*C*Mepz$_2$), 24.8 ppm (Me); LR-MS (ESI$^+$): *m*/*z* (%): 375 (100) [*M*$^+$−2Cl−H]; ele-

mental analysis calcd (%) for $C_{14}H_{14}Cl_2N_4O_2Pd$ (447.61): C 37.57, H 3.15, N 12.52; found: C 37.51, H 3.29, N 12.64.

Synthesis of 12_{ox}: Neat [$PdCl_2$(cod)] (0.031 g, 0.11 mmol) was added to a solution of 11_{ox} (0.030 g, 0.11 mmol) in CH_3CN (5 mL) at room temperature. After the resulting mixture had been stirred for 48 h at room temperature, all of the volatiles were removed in vacuo. The yellow solid residue of 12_{ox} was first washed with CH_2Cl_2 (1 mL) and then with hexane (10 mL) to give the final product (0.029 g, 59%). Single crystals of 12_{ox} formed upon gas-phase diffusion of Et_2O into a saturated solution of 12_{ox} in CH_3CN. ^{1}H NMR (250.1 MHz, CD_3CN): δ = 8.23, 7.96 (m, br, 2×2H; pzH-3,5), 6.97 (dd, ^3J(H,H) = 10.2 Hz, ^4J(H,H) = 2.4 Hz, 1H; BQH-5), 6.83 (d, ^3J(H,H) = 10.2 Hz, 1H; BQH-6), 6.57 (m, 2H; pzH-4), 5.80 (d, ^4J(H,H) = 2.4 Hz, 1H; BQH-3), 2.68 ppm (s, 3H; Me); ^{13}C NMR (62.9 MHz, CD_3CN): δ = 187.3, 185.1 (BQC-1,4), 145.7 (br, pzC-3 or pzC-5), 145.4 (BQC-2), 138.7 (BQC-6), 137.4 (BQC-5), 137.0 (BQC-3), 134.7 (br, pzC-5 or pzC-3), 108.5 (pzC-4), 79.9 ($CMepz_2$), 23.8 ppm (Me); LR-MS (ESI$^+$): m/z (%): 450 (100) [M^+−Cl+CH_3CN]; elemental analysis calcd (%) for $C_{14}H_{12}Cl_2N_4O_2Pd$ (445.60): C 37.74, H 2.71, N 12.57; found: C 37.65, H 2.95, N 12.40.

Crystal structure determinations of 5, 6, 7 and 12_{ox}: Crystals of **5** and **6** were measured by using a Siemens SMART 1*K*-CCD diffractometer with graphite-monochromated $Mo_{K\alpha}$ radiation. An empirical absorption correction was performed for **5** by using the SADABS[55] program and a numerical absorption correction was performed for **6**. Data for **7** and 12_{ox} were collected by using a Stoe-IPDS-II two-circle diffractometer with graphite-monochromated $Mo_{K\alpha}$ radiation. Empirical absorption corrections were performed by using the MULABS option[56] in the PLATON[57] program. All of the structures were solved by direct methods[58] and refined by full-matrix least-squares methods on F^2 by using the SHELXL97[59] program. Hydrogen atoms were placed at ideal positions and refined with fixed isotropic displacement parameters by using a riding model. The unit cell of **5** contains two symmetry-related solvent accessible areas of about 479 Å^3 each which contain completely disordered solvate. The PLATON/SQUEEZE[57] program was used to account for the solvent electron density. Complex **7** crystallises with four molecules of CH_3CN in the asymmetric unit whereas complex 12_{ox} crystallises with one molecule of CH_3CN in the asymmetric unit.

CCDC 663883 (**2a**), 663884 ($2b_{ox}$), 663885 (**2c**), 663886 (**4**·DMF_2), 663887 (**5**), 663888 (**6**), 662352 (**7**), 662354 (**9**), 662353 (12_{ox}) and 662355 (**13**) contain the supplementary crystallographic data for this paper. These data can be obtained free of charge from the Cambridge Crystallographic Data Centre via www.ccdc.cam.ac.uk/data_request/cif

Electrochemical measurements: All of the electrochemical measurements were performed by using an EG&G Princeton Applied Research 263A potentiostat with glassy carbon (**11**, 11_{ox}, **12**, **13**) or platinum disc (12_{ox}) working electrodes. Carefully dried (CaH_2) and degassed CH_3CN was used as the solvent and [NBu_4]PF_6 as the supporting electrolyte (0.1 M). All potential values are referenced against the FcH/FcH$^+$ couple.

Acknowledgements

The authors are grateful to the Deutsche Forschungsgemeinschaft (DFG) and the Fonds der Chemischen Industrie (FCI) for financial support.

[1] M. D. Ward, J. A. McCleverty, *J. Chem. Soc., Dalton Trans.* **2002**, 275–288.
[2] W. Kaim, B. Schwederski, *Pure Appl. Chem.* **2004**, *76*, 351–364.
[3] M. D. Ward, *Chem. Soc. Rev.* **1995**, *24*, 121–134.
[4] V. Balzani, A. Juris, M. Venturi, S. Campagna, S. Serroni, *Chem. Rev.* **1996**, *96*, 759–833.
[5] K. Ma, M. Scheibitz, S. Scholz, M. Wagner, *J. Organomet. Chem.* **2002**, *652*, 11–19.
[6] F. Jäkle, K. Polborn, M. Wagner, *Chem. Ber.* **1996**, *129*, 603–606.
[7] F. Fabrizi de Biani, F. Jäkle, M. Spiegler, M. Wagner, P. Zanello, *Inorg. Chem.* **1997**, *36*, 2103–2111.
[8] E. Herdtweck, F. Peters, W. Scherer, M. Wagner, *Polyhedron* **1998**, *17*, 1149–1157.
[9] S. L. Guo, F. Peters, F. Fabrizi de Biani, J. W. Bats, E. Herdtweck, P. Zanello, M. Wagner, *Inorg. Chem.* **2001**, *40*, 4928–4936.
[10] A. Haghiri Ilkhechi, M. Scheibitz, M. Bolte, H.-W. Lerner, M. Wagner, *Polyhedron* **2004**, *23*, 2597–2604.
[11] A. Haghiri Ilkhechi, M. Bolte, H.-W. Lerner, M. Wagner, *J. Organomet. Chem.* **2005**, *690*, 1971–1977.
[12] A. Haghiri Ilkhechi, J. M. Mercero, I. Silanes, M. Bolte, M. Scheibitz, H.-W. Lerner, J. M. Ugalde, M. Wagner, *J. Am. Chem. Soc.* **2005**, *127*, 10656–10666.
[13] Ditopic neutral phenylene-bridged bis(pyrazol-1-yl)methane ligands have been reported by Reger et al., see: a) D. L. Reger, R. P. Watson, M. D. Smith, P. J. Pellechia, *Organometallics* **2005**, *24*, 1544–1555; b) D. L. Reger, R. P. Watson, M. D. Smith *Inorg. Chem.* **2006**, *45*, 10077–10087.
[14] P. Chaudhuri, C. N. Verani, E. Bill, E. Bothe, T. Weyhermüller, K. Wieghardt, *J. Am. Chem. Soc.* **2001**, *123*, 2213–2223.
[15] H.-W. Lerner, G. Margraf, T. Kretz, O. Schiemann, J. W. Bats, G. Dürner, F. Fabrizi de Biani, P. Zanello, M. Bolte, M. Wagner, *Z. Naturforsch.* **2006**, *61b*, 252–264.
[16] R. Dinnebier, H.-W. Lerner, L. Ding, K. Shankland, W. I. F. David, P. W. Stephens, M. Wagner, *Z. Anorg. Allg. Chem.* **2002**, *628*, 310–314.
[17] B. Wolf, S. Zherlitsyn, B. Lüthi, N. Harrison, U. Löw, V. Pashchenko, M. Lang, G. Margraf, H.-W. Lerner, E. Dahlmann, F. Ritter, W. Assmus, M. Wagner, *Phys. Rev. B* **2004**, *69*, 092403.
[18] G. Margraf, T. Kretz, F. Fabrizi de Biani, F. Laschi, S. Losi, P. Zanello, J. W. Bats, B. Wolf, K. Remović-Langer, M. Lang, A. Prokofiev, W. Assmus, H.-W. Lerner, M. Wagner, *Inorg. Chem.* **2006**, *45*, 1277–1288.
[19] H. O. Jeschke, L. A. Salguero, R. Valentí, C. Buchsbaum, M. U. Schmidt, M. Wagner, *C. R. Chim.* **2007**, *10*, 82–88.
[20] B. Wolf, A. Brühl, V. Pashchenko, K. Remović-Langer, T. Kretz, J. W. Bats, H.-W. Lerner, M. Wagner, A. Salguero, T. Saha-Dasgupta, B. Rahaman, R. Valentí, M. Lang, *C. R. Chim.* **2007**, *10*, 109–115.
[21] G. Margraf, J. W. Bats, M. Bolte, H.-W. Lerner, M. Wagner, *Chem. Commun.* **2003**, 956–957.
[22] T. Kretz, J. W. Bats, S. Losi, B. Wolf, H.-W. Lerner, M. Lang, P. Zanello, M. Wagner, *Dalton Trans.* **2006**, 4914–4921.
[23] T. Nikuni, M. Oshikawa, A. Oosawa, H. Tanaka, *Phys. Rev. Lett.* **2000**, *84*, 5868–5871.
[24] T. M. Rice, *Science* **2002**, *298*, 760–761.
[25] Ch. Rüegg, N. Cavadini, A. Furrer, H.-U. Güdel, K. Krämer, H. Mutka, A. Wildes, K. Habicht, P. Vorderwisch, *Nature*, **2003**, *423*, 62–65.
[26] C. Pettinari, R. Pettinari, *Coord. Chem. Rev.* **2005**, *249*, 663–691.
[27] T. Kretz, J. W. Bats, H.-W. Lerner, M. Wagner, *Z. Naturforsch.* **2007**, *62b*, 66–74.
[28] T. C. Higgs, C. J. Carrano, *Inorg. Chem.* **1997**, *36*, 291–297.
[29] J. P. Klinman, D. Mu, *Annu. Rev. Biochem.* **1994**, *63*, 299–344.
[30] M. Mure, J. P. Klinman, *J. Am. Chem. Soc.* **1995**, *117*, 8707–8718.
[31] J. P. Klinman, *Chem. Rev.* **1996**, *96*, 2541–2561.
[32] P. Li, N. K. Solanki, H. Ehrenberg, N. Feeder, J. E. Davies, J. M. Rawson, M. A. Halcrow, *J. Chem. Soc., Dalton Trans.* **2000**, 1559–1565.
[33] J.-E. Bäckvall, R. B. Hopkins, H. Grennberg, M. M. Mader, A. K. Awasthi, *J. Am. Chem. Soc.* **1990**, *112*, 5160–5166.
[34] V. Busico, P. Corradini, L. Landriani, M. Trifuoggi, *Makromol. Chem. Rapid Commun.* **1993**, *14*, 261–266.
[35] P. W. N. M. van Leeuwen, *Homogeneous Catalysis. Understanding the Art*, Kluwer, Dordrecht, **2004**.
[36] M. D. K. Boele, G. P. F. van Strijdonck, A. H. M. de Vries, P. C. J. Kamer, J. G. de Vries, P. W. N. M. van Leeuwen, *J. Am. Chem. Soc.* **2002**, *124*, 1586–1587.
[37] N. Ma, Z. Duan, Y. Wu, *J. Organomet. Chem.* **2006**, *691*, 5697–5700.

[38] D. D. Hennings, T. Iwama, V. H. Rawal, *Org. Lett.* **1999**, *1*, 1205–1208.
[39] T. C. Higgs, K. Spartalian, C. J. O'Connor, B. F. Matzanke, C. J. Carrano, *Inorg. Chem.* **1998**, *37*, 2263–2272.
[40] M. Mure, J. P. Klinman, *J. Am. Chem. Soc.* **1995**, *117*, 8698–8706.
[41] K. I. The, L. K. Peterson, *Can. J. Chem.* **1973**, *51*, 422–426.
[42] K. I. The, L. K. Peterson, E. Kiehlman, *Can. J. Chem.* **1973**, *51*, 2448–2451.
[43] L. K. Peterson, E. Kiehlman, A. R. Sanger, K. I. The, *Can. J. Chem.* **1974**, *52*, 2367–2374.
[44] A. Otero, J. Fernández-Baeza, J. Tejeda, A. Antiñolo, F. Carrillo-Hermosilla, E. Díez-Barra, A. Lara-Sánchez, M. Fernández-López, M. Lanfranchi, M. A. Pellinghelli, *J. Chem. Soc., Dalton Trans.* **1999**, 3537–3539.
[45] M. Hesse, H. Meier, B. Zeeh, *Spektroskopische Methoden in der organischen Chemie*, Thieme, Stuttgart, **1987**.
[46] T. C. Higgs, C. J. Carrano, *Inorg. Chem.* **1997**, *36*, 298–306.
[47] S. Tsuji, D. C. Swenson, R. F. Jordan, *Organometallics* **1999**, *18*, 4758–4764.
[48] A. Mentes, R. D. W. Kemmitt, J. Fawcett, D. R. Russeli, *Polyhedron* **1999**, *18*, 1141–1145.
[49] D. J. Tempel, L. K. Johnson, R. L. Huff, P. S. White, M. Brookhart, *J. Am. Chem. Soc.* **2000**, *122*, 6686–6700.
[50] S. R. Ananias, A. E. Mauro, K. Zutin, C. M. C. Picchi, R. H. A. Santos, *Transition Met. Chem. (Dordrecht Neth.)* **2004**, *29*, 284–290.
[51] M. Bauscher, W. Mäntele, *J. Phys Chem.* **1992**, *96*, 11101–11108.
[52] R. C. Prince, P. L. Dutton, J. M. Bruce, *FEBS Lett.* **1983**, *160*, 273–276.
[53] M. Bauscher, E. Nabedryk, K. Bagley, J. Breton, W. Mäntele, *FEBS Lett.* **1990**, *261*, 191–195.
[54] J. M. Ready, E. N. Jacobsen, *J. Am. Chem. Soc.* **2001**, *123*, 2687–2688.
[55] G. M. Sheldrick, SADABS, Universität Göttingen, Göttingen (Germany), **2000**.
[56] R. H. Blessing, *Acta Crystallogr., Sect. A* **1995**, *51*, 33–38.
[57] A. L. Spek, *Acta Crystallogr., Sect. A* **1990**, *46*, C34.
[58] G. M. Sheldrick, *Acta Crystallogr., Sect. A* **1990**, *46*, 467–473.
[59] G. M. Sheldrick, SHELXL-97, A Program for the Refinement of Crystal Structures, Universität Göttingen, Göttingen (Germany), **1997**.

Received: October 12, 2007
Published online: January 10, 2008

